J. Materials, Conc. Struct., Pavements No. 532/V-30, 183-195, February 1996

EMBEDDED BAR BEHAVIOR IN CONCRETE UNDER COMBINED AXIAL PULLOUT AND TRANSVERSE DISPLACEMENT

Koichi MAEKAWA[1] and Juneid QURESHI[2]

[1] Member of JSCE, Dr. of Eng., Associate Prof., Dept. of Civil Eng., the University of Tokyo (Hongo 7-3-1, Bunkyo-ku, Tokyo 113, Japan)
[2] Dr. of Eng., Assistant Prof., NED University of Engineering & Technology (Karachi, Pakistan)

This paper investigates pullout behavior of embedded deformed bars in concrete under coupled transverse shear arising at a crack of reinforced concrete. It was experimentally proven that the pullout capacity, which reaches yield of steel section at a crack under uniaxial tension, does not come up with full yielding of the critical section where the axial stress gets maximum, but the ultimate limit state is reached not at the RC crack plane but inside location in which induced curvature by shear slip of crack takes place. It is concluded under higher reinforcement ratio and/or flatter planes of concrete joints, coupling of pullout and transverse shear of steel at a crack cannot be ignored in structural analysis.

Key Words : *dowel action, bond, crack, reinforcement, joint interface*

1. INTRODUCTION

Recent development in predicting structural concrete behavior has been performed by enhancing constitutive laws of reinforced concrete[1]. Among them, the bond behavior gets primary position since major nonlinearity of RC members originates from crack planes reinforced by deformed bars. Macroscopic aspects of bond have been mechanically expressed in terms of tension stiffening of concrete and pullout of embedded bars from concrete[2]. These computational models have been applied to both discrete and smeared crack elements in the frame of nonlinear finite element analysis[1].

In general, the stress of bars at crack planes are computed only with respect to pullout slip geometrically defined *along the axis of bars*. The presence of transverse displacement to the axis of bars is not taken into account for computing axial stress - pullout relation, and the applicability of this hypothesis which brings about simplicity of computation was carefully examined by Mishima et al[4]. Through this series of experimental verification, it was clarified that reinforced concrete normal cracks, which are introduced by tension stress in concrete and reinforced by deformed bars of reinforcement ratio not greater than 2%, can be successfully dealt with by the simple superposition law of stress transfer of concrete crack[11], and the bond-slip model of a single reinforcing bar [2].

However, it was simultaneously manifested that the simple superposition law brings the overestimated shear capacity of reinforced concrete crack planes and higher shear stiffness than reality when the higher reinforcement ratio is provided[5]. According to the recent development of enhanced micro-mechanical constitutive modeling[11),12)], this tendency has been getting more and more clear. For heavily reinforced crack and/or joint planes with smoother configuration of surfaces, the reduction of confinement efficiency by reinforcing bars crossing shear planes was raised owing to coupled displacement paths consisting of transverse displacements and axial pullout [5),13)].

At present, no convincing experimental proof, which can be used also for computational models, is supplied. This paper deals with behaviors of embedded deformed reinforcing bars under coupled interface opening and transverse shear displacement, and both macro and micro-mechanical aspects are carefully discussed. The main attention is paid to the axial mechanical performance of an embedded reinforcing bar under the presence of the coupled dowel action of the bar. In this study, the reinforcing bar is treated not as a one-dimensional cord but as three-dimensional body.

Table 1 Dimensions, mechanical and material properties and types of interfaces for specimens tested

specimen	b*h(mm)	p (%)	fy (MPa)	D (mm) center	D (mm) side	fc' (MPa)	concrete type	Joint type
1	150*300	1.18	446	25	none	40	NC	RC
2	200*300	2.24	446	25	16(4bars)	41	NC	RC
3	200*300	4.44	403	25	25(4bars)	48	NC	RC
4	150*300	1.57	480	25	none	40	HPC	U-CJ
5	150*200	0.95	450	13	13(2bars)	35	HPC	U-CJ
6	150*200	1.58	450	13	13(4bars)	35	HPC	U-CJ
7	150*150	1.84	360	16	16(1-bar)	50	HPC	P-CJ
8	150*150	0.95	360	16	none	43	HPC	U-CJ
9	150*150	0.95	360	16	none	42	HPC	P-CJ
10	150*150	0.95	360	16	none	27	NC	U-CJ
11	150*150	0.95	360	16	none	28	NC	P-CJ

/b*h : width and height of the section /p : reinforcement ratio /fy : yield strength of the bars /fc' : compressive strength of concrete
/Specimens 4, 5, 6 and 7 are instrumented with strain gages along their axis; all other specimens instrumented with strain gages only at the interface.
/Bar arrangement is symmetric in cross section for all specimens as illustrated in Fig.3.
/NC : normal concrete /HPC: self-compacting concrete /U : unprocessed /P : tipping process /RC : rough crack /CJ : construction joint

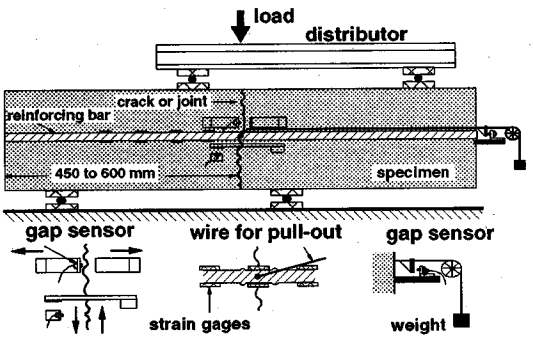

Fig.1 Test set-up and instrumentation

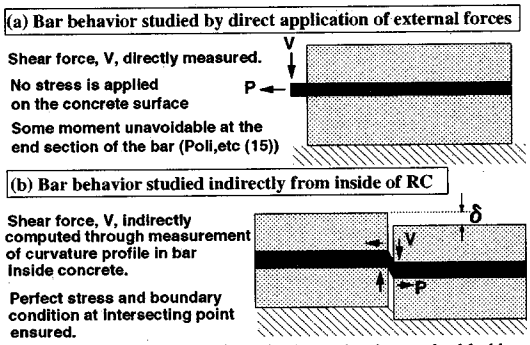

Fig.2 Schematic arrangement for investigating embedded bar behavior.

2. PULLOUT TESTS OF EMBEDDED BAR UNDER COUPLED TRANSVERSE SHEAR

(1) Specimens and loading

The coupled pullout and transverse shear displacement paths were introduced to a reinforcing bar at a crack by conducting pure shear loading adopted on a beam type specimen as shown schematically in **Fig.1**. The interface opening denoted by ω_s was measured at two places on each face of a specimen, and the transverse displacement defined as δ was measured at the mid-depth of each face. The pullout (denoted by S and defined as bar axial displacement measured based on the concrete point of far field[2]) at the center of the interface section was picked up by the gap sensor directly through a stainless steel wire inserted in a plastic tube as shown in **Fig.1**. Here, the far field point was set at the concrete surface on which the gap sensor was attached.

The plastic tube was adhered to the bar at several locations and wax was applied along its length for debonding with concrete and to ensure free movement of the tube with the bar undergoing transverse displacement. The sectional stress of a reinforcing bar at an interface, where shear slip was induced, was obtained by measuring strain and utilizing predefined stress-strain relation of the bar concerned. The embedded length of the bar was provided greater than '25D' (Let D denote bar diameter) so that sufficient anchorage can be guaranteed and free end slip of bars gets negligible[2]. The specimens were loaded monotonically to failure. Details of specimen dimensions, mechanical properties, bar arrangement, material properties and interface types are listed in **Table 1**.

The test set-up and loading arrangement chosen in this study have inherent advantages and disadvantages. As shown in **Fig.2**, another possible test set-up would be to directly apply axial load P and transverse shear V to a bar. The advantage in this case is that any type of load history can be

controlled. Contrary, it is difficult to reproduce real boundary conditions. Bending moment of the bars must be zero at the interface, but cannot be guaranteed here. In fact, compressive confining stress is applied on the rough crack surface around the bars owing to shear dilatancy mechanism, but type (a) method in **Fig.2** produces perfectly zero confinement.

Concerning the approach chosen for this study, although it is impossible to obtain the transverse force directly nor free control of load paths, perfect boundary condition is ensured at the intersecting point. The strategy of this approach is to pick up information from inside of reinforced concrete, regarding embedded bars in an stable manner as possible. Also, the transverse force carried by the bar, although not directly measured, can be computed provided that the associated bending moment along the bar axis is known as discussed in later section.

The tension force applied to the bar originates from the interface dilatancy associated with the transverse shear. The important point is that the bar at the interface is subjected to the generic condition of coupled pullout and transverse displacement which were measured along the interface. The axial force induced in the bar was controlled by intentionally changing geometrical profiles of crack planes as well as by placing additional reinforcement around the target bar, thereby changing reinforcement ratio.

The rough crack, which makes the crack gap wider, was introduced by splitting tension force and the associated roughness was generated. The flat plane which induces smaller interface opening coupled with shear slip was also reproduced by constructing concrete on the surface of previously cast concrete construction joint. By the above stated method, successful reproductions of different pullout denoted by S ($\equiv\omega_s/2$) versus transverse shear ($=\delta/2$) paths to the embedded bar at the interface was experimentally simulated with wider range. These tests were fundamentally carried out to study behaviors of reinforcing bars embedded in concrete.

(2) Pullout affected by transverse shear

The pullout slip versus mean axial stress of typical specimens at interfaces are shown in **Fig.3**. Notations in these figures are the same as those defined in **Table 1**. The uniaxial pullout behavior, which was obtained under axial pullout only and fairly predicted by the model of Shima et al.[2], is also shown as a referential case in **Fig.3**. Under pure axial pullout, the pullout stiffness is close to zero when the stress of reinforcing bars at the crack comes up to the yield strength of the bar, because the plastic range penetrates from the crack point into the steel section inside concrete. As reported by Mishima et al.[7], the common pullout behavior can be seen even under coupled displacement paths of axial pullout with the transverse shear along a crack.

However, the pullout stiffness is reduced even when the axial stress is lower than the yield strength as shown in **Fig.3**. The initiating point of the reduced stiffness is directly influenced by the field of induced displacement path. Higher ratios of transverse displacement to axial pullout induces earlier initiation of deviation from the pure axial pullout stiffness, as can be seen in **Fig.3(a,c)**. Also the maximum confining stress provided by embedded bars at a crack section, $\sigma_{s,ult}$, which determines the ultimate shear capacity, is much less than the uniaxial capacity of bare steel bars represented by f_y.

At the crack section, steel was examined to be still elastic despite of the inelastic pullout from concrete. When the crack opening was more confined by additional reinforcement, significant reduction in anchorage performance represented by $\sigma_{s,ult}$ was detected. But the elasticity of the steel at the crack section was verified. Reduction in mean yield strength, defined as the axial capacity under coupled shear and pullout from the uniaxial yield strength of the steel, varied from 22% for lightly reinforced sections, Specimen 1 (p=1.2%, with one 25mm diameter bar), to as much as 67% for heavily reinforced sections, Specimen 3 (p=4.4%, with five 25mm diameter bars), as seen in **Fig.3(a,c).**

This reduction rate was also checked by changing displacement paths. Some specimens were tested with crack planes designed as a construction joint as explained earlier. The smooth crack asperity, and the resultant high transverse displacement to crack opening ratio induced, exhibited more significant reduction in the mean yield strength of the bar, even at low reinforcement ratios, with about 39% reduction for Specimen 5 (p=0.95%, with three 13mm diameter bars) and about 47% for Specimen 6 (p=1.58%, with five 13mm diameter bars) as shown in **Fig.3(e,f)**. Specimen 5 shows larger reduction than Specimen 1, even though reinforcement ratio is smaller. This is thought to be caused by smoother interface.

In the case of Specimen 10 with normal concrete unprocessed construction joint, a very steep displacement path in terms of bar transverse displacement to axial pullout is observed and the mean yield strength is reduced by as much as 56% even though p=0.95% only as shown in **Fig.3(h).**

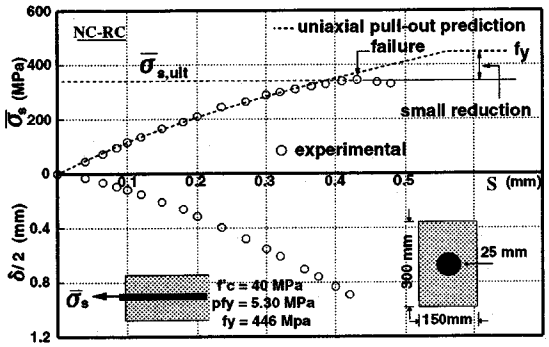

(a) : Specimen 1

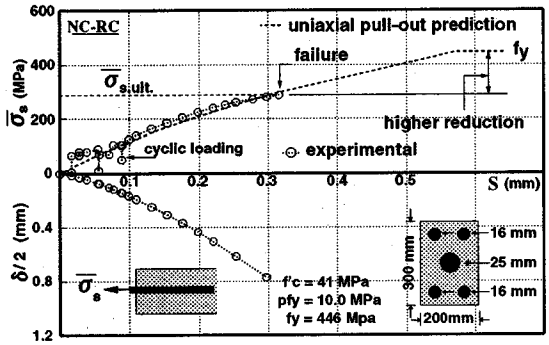

(b) : Specimen 2

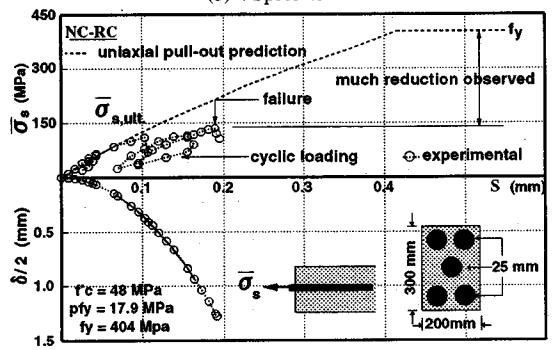

(c) : Specimen 3

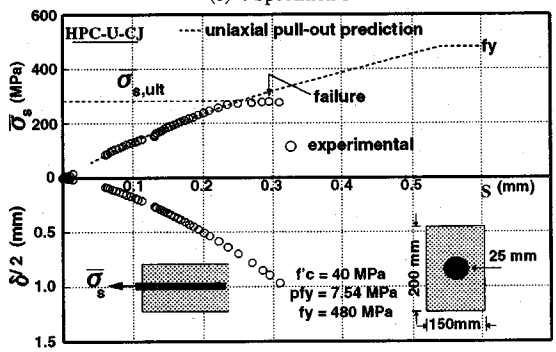

(d) : Specimen 4

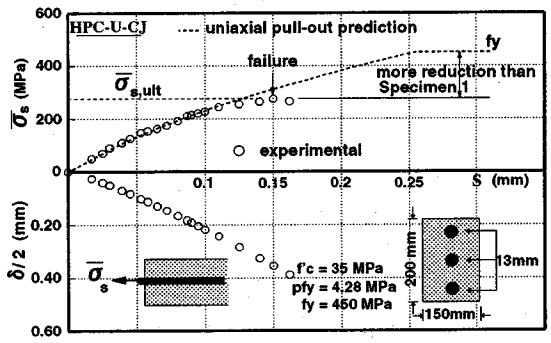

(e) : Specimen 5

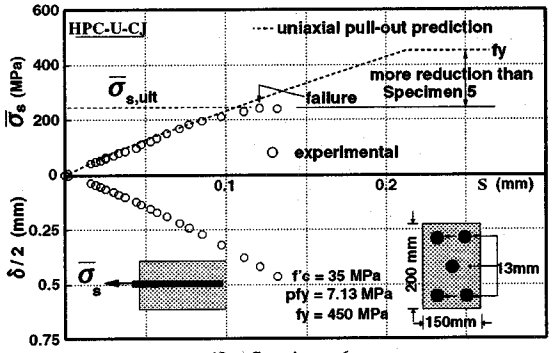

(f) : Specimen 6

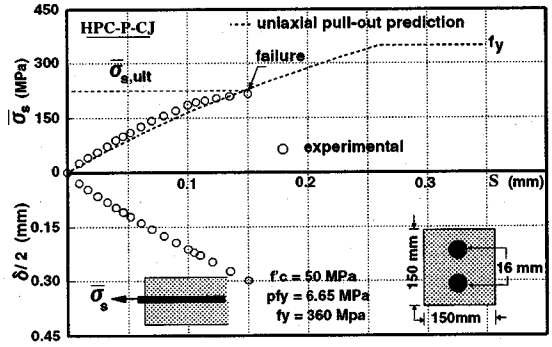

(g) : Specimen 7

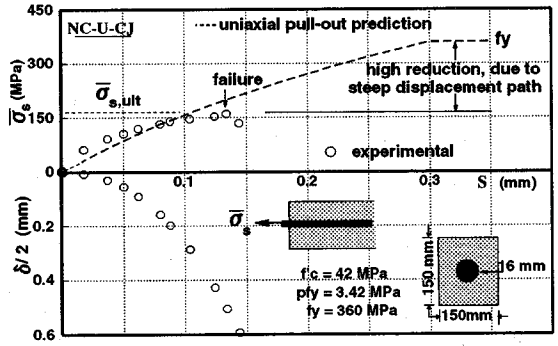

(h) : Specimen 10

Fig.3 Mean axial stress at interface with associated axial pullout and transverse displacement, for rough cracks and construction joints.

From these results, it can be concluded that the pullout behavior deviates from that obtained under the pure axial tension, to which broad attention has been paid in the past research[8]. Furthermore, higher the ratio of the transverse displacement to the crack opening, brought about by higher reinforcement

ratio, flatter interface surface geometry or lower concrete strength, the lower is the capacity of the anchorage. In the past, the shear failure of concrete crack plane was reported [14] as the counterpart of yielding failure of reinforcement at a crack. According to the reduced axial stiffness and steel confinement, the shear failure mode, which was supposed being associated with the failure of crack plane, needs to be re-examined in detail.

3. MECHANISM OF REDUCED AXIAL PERFORMANCE BY COUPLED SHEAR

(1) Local yield of steel inside concrete

Since the flatter plane with less dilatancy facilitates much reduction of pullout stiffness, the microscopic mechanism associated with this reduced stiffness and capacity was investigated as shown in **Fig.4**. As the reduced capacity of pullout resistance will be rooted in local plasticity arising in embedded steel bars, profiles of the local curvature and mean axial strains were locally measured. Grooved bars were utilized to fix strain gages in order to maintain the local bond. Measurements were taken along the bar from the joint plane up to sufficient embedded length, defined as a control section, of up to 8 to 10 times the bar diameter beyond which the effect of the crack shear displacement became negligible. The flat plane was obtained by concreting above already hardened concrete block, with a concreting time separation of at least 24 hours.

The relations between the mean axial bar stress at the joint versus the pull-out at the joint, locally measured on the bar, and the associated transverse displacement of the bar, are shown in **Fig.3(d, e, f and g)**, along with similar results for rough cracks. It can be seen in **Fig.3** that in the initial stages the pullout behavior is close to the uniaxial one, but in most cases it deviates from this behavior as the transverse displacement goes on increasing. It is also seen that the axial capacity reached by the bar is less than the axial yield capacity, as determined from tests of bare steel bars, uniaxially pulled[2].

The profile of the mean axial stress, mean axial strain and induced curvature, along the bar axis for typical specimens, are shown in **Fig.5**. The axial sectional mean strain defined as ε_s and the curvature $\phi(x)$ were obtained by measuring the local strains on top and bottom of the grooved section (ε_t, ε_b) at discrete intervals (See **Fig.4**).

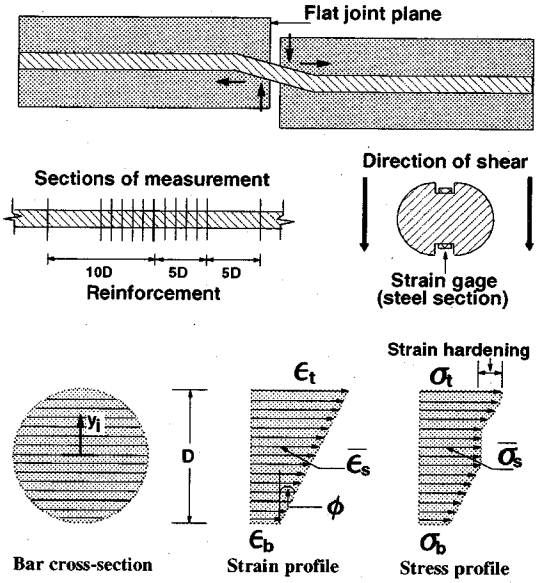

Fig.4 Discretization of reinforcing bars

$$\phi(x)=\frac{\varepsilon_t-\varepsilon_b}{D} \quad \bar{\varepsilon}_s(x)=\frac{\varepsilon_t+\varepsilon_b}{2} \tag{1}$$

where, D denotes the bar diameter.

The mean axial stress, which is sectionally averaged, is computed by assuming the plane section remaining plane hypothesis as,

$$\bar{\sigma}_s(x)=\frac{1}{A_s}\int_{-D/2}^{+D/2}\sigma_s(\varepsilon_s)dA_s$$
$$\varepsilon_s(x,y)=\bar{\varepsilon}_s(x)+\phi(x)\cdot y \tag{2}$$

where, "y" is the local coordinate along the bar section, measured from the sectional centroid, and dAs is the y-derivative strip of the cross-sectional area along the bar section into which it is divided and As is the cross-sectional area.

Notation σ_s denotes the fiber stress and was obtained from the uniaxial stress strain relation of the bar used as,

$$\sigma_s=E_s\cdot\varepsilon_s \quad :0<\varepsilon_s<\varepsilon_y$$
$$\sigma_s=f_y \quad :\varepsilon_y\le\varepsilon_s<\varepsilon_{sh}$$
$$\sigma_s=f_y\{1-\exp(\varepsilon_{sh}-\varepsilon_u)/k\}\cdot(1.01f_u-f_y) \tag{3}$$
$$k=0.047(400/f_y)^{2/3}, \quad \varepsilon_{sh}\le\varepsilon_s<\varepsilon_u$$

where, f_y, f_u, ε_y and ε_u are the yield and tensile strength and corresponding strains, respectively, ε_{sh} is the strain at onset of strain hardening and E_s is the initial elastic modulus of the bar. A numerical solution technique to determine the local axial stress from the local axial strain profile across a circular

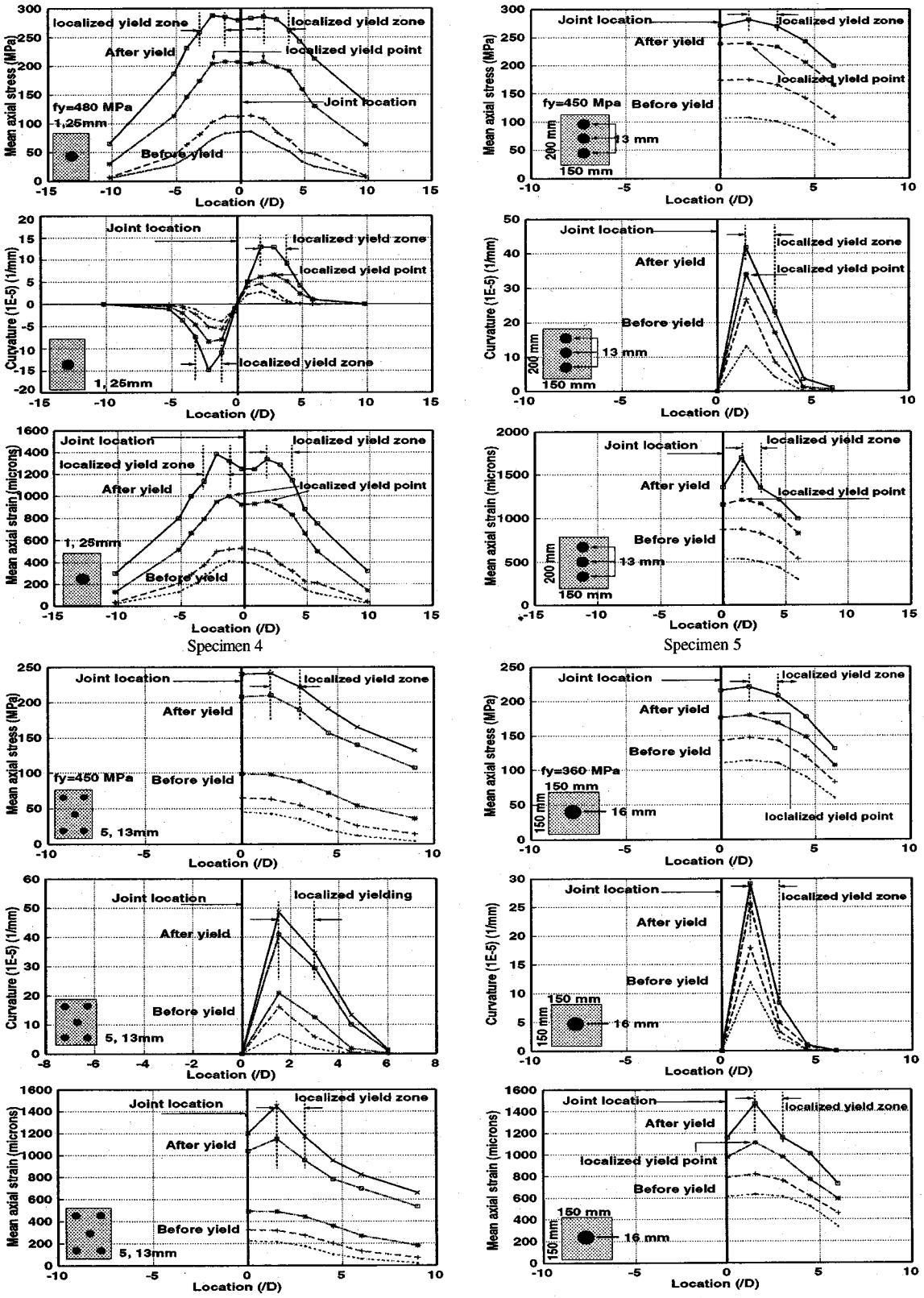

Fig.5 Profiles of mean axial stress, strain and curvatures along an axis of reinforcing bars

section, by discretizing the bar section in finite number of strips and using a predefined stress-strain relation for the bar, is shown in **Fig.4**.

In **Fig.3**, it can be seen that in the range where the axial stiffness is prominently reduced, the steel inside concrete must have yielded to explain the non-linearity, in spite of the experimental fact that the section at the crack is still in elasticity. The mechanism for this phenomenon can be understood from **Fig.5**. The axial mean stress of the bar near the joint plane is quite smooth and relatively uniform very close to the crack, indicating loss of local bond[2].

But the profile for the axial mean strain is more complex, exhibiting local non-uniformity or 'jumps', near the joint plane as shown in **Fig.5**. The maximum strain in the bar occurs inside the concrete at a location depending on the bar diameter, typically around 2D form the joint plane. The profile for the mean axial strain follows the profile of the local curvature witnessed in the bar, which is also dependent on the bar diameter, typically between 4D to 5D.

Here, with increasing transverse displacement, the length of the curvature profile shows small increments, with basically the similar distribution profile. Since the integral of the mean axial strain with respect to the location along bar is equal to the pullout measured at the crack, the effect of the observed reduced axial stiffness on pullout can be attributed to this non-uniformity in the mean axial strain.

In the experiments it was clearly observed that localized yielding occurs in the extreme bar fibers inside concrete according to the strain measurements done in the tests. However the section at the interface remains fully elastic. The yield sections shown in **Fig.5** indicate partial yielding of the bar cross-section and not full yield of the entire section. It is this partial yielding associated with the local curvature which causes the loss of mechanical axial stiffness and the corresponding additional inelastic elongation along the axis.

(2) Associated transverse shear and local yield of reinforcing bars

The source of the plasticity arising at the internal section is the local curvature induced by the transverse displacement. The sectionally averaged mean axial stress-strain profile at the crack section and at the maximum curvature location, for some typical specimens, are shown in **Fig.6**. Under the small crack opening and transverse displacement, the entire fibers remain elastic at both locations. This corresponds to the initial part of the steel stress at crack versus pullout relations, as the mean axial stress-strain relation coincides with the constitutive law of a bare bar uniaxially pulled[7].

However, with increased transverse displacement, the curvature goes on increasing owing to deformational compatibility, till the extreme fiber comes up to the local yield strain. The qualitative local sectional stress profiles of the bar, at the ultimate shear capacity of the interface are also shown in **Fig.6**.

This localized yielding initiates the reduction in axial stiffness, as shown in **Fig.7**, which depicts the sectionally averaged mean stress-strain relation for a bar with bending, represented by varying levels of constant curvature values, and axial force. Also represented in this figure is a general criteria for the failure condition of the bar under interactive stresses, expressed by a functional relationship in terms of ratios of the actual forces to the strength, under pure axial and bending forces.

The maximum possible interactive stress in the bar under such conditions, computed on the basis of plane section theory of beams, is expressed by the interaction failure surface[16], defined by,

$$\left[\frac{P(x)}{P_o}\right]^2+\left[\frac{M(x)}{M_o}\right]=1 \qquad (4)$$

where, $P(x)$ and $M(x)$ are the local axial force and bending moment along the bar axis, respectively, and P_o and M_o are the capacities under pure axial tension and bending. The derivation of such an equation requires knowledge of the stress-strain relationship of the material (which is idealized here as rigid-plastic), definition of capacity in terms of limiting stress or strain (considered here as axial yield stress of the bar, f_y), and a solution of two equilibrium conditions for the given cross section, that is,

$$\begin{aligned}\int_{-D/2}^{D/2}\sigma_s(x,y)dA_s(y)&=P(x)\\ \int_{-D/2}^{D/2}\sigma_s(x,y)\cdot y\cdot dA_s(y)&=M(x)\end{aligned} \qquad (5)$$

It is clear from **Fig.7** that the greater the curvature, or bending moment producing the curvature, across a section, the more is the reduction of axial stiffness. Also the maximum axial stress that is attained becomes lower with the increase in curvature. As seen from test results, when an embedded bar is subjected to a coupled displacement path, the local

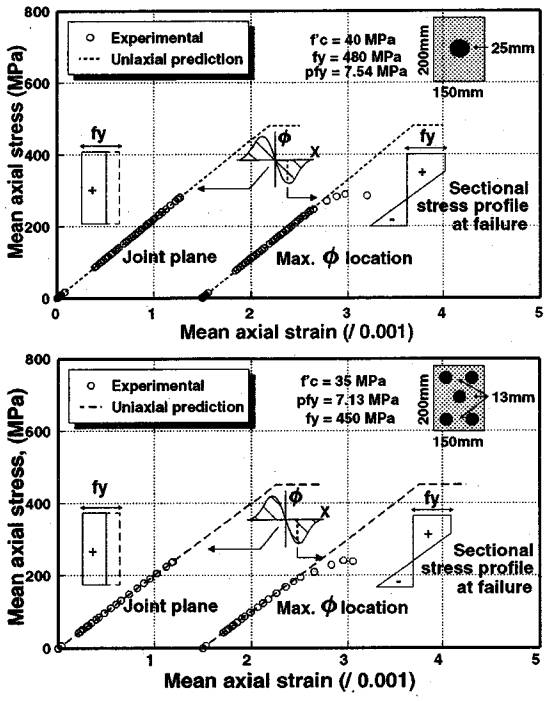

Fig.6 Sectionally averaged mean axial stress-strain relations at interface and maximum curvature location (upper : Specimen 4, lower : Specimen 6).

maximum curvature does not remain constant but increases with the increase in bar transverse displacement. Hence, the actual mean axial stress-strain path followed by the bar would be as shown through the arrow headed line in **Fig.7**.

(3) Influencing factors for localized yield of steel

In the case of heavily reinforced sections or smooth crack surface geometry, the transverse displacement associated with corresponding bar pullout becomes higher, in order to satisfy the equilibrium of force condition normal to the crack plane. The higher transverse displacement induces higher curvature, as compatibility requires that the double integral of the curvature profile equals the transverse bar displacement, if shear deformations are negligible. The higher curvature then initiates the reduced axial stiffness and also determines the maximum bar strength when subjected to simultaneous bending and axial forces. This is clear from the mean axial stress and curvature profiles for specimens 5 and 6, which have the same bar diameter, as shown in **Fig.5**. Specimen 6 which has the higher reinforcement ratio

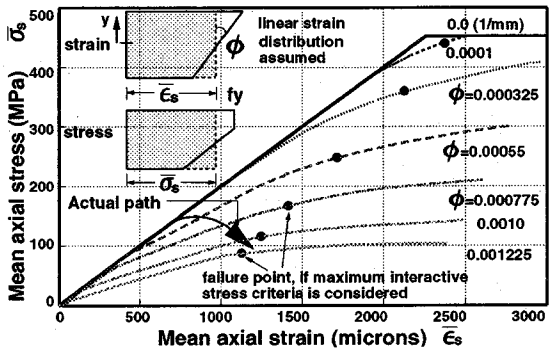

Fig.7 Effect of curvature on mean axial stress-strain relation of bar based on plane section theory.

than Specimen 5, has higher induced curvature and a lower mean axial stress of the bar at failure.

Although the effect of increased reinforcement ratio on bar axial stiffness and strength is very significant, the effect of bar diameter is quite complicated. Several interactive parameters determine the overall effect of bar diameter on the reduced axial stiffness and capacity of reinforcing bars at a crack or joint plane. This is because although the bigger diameter bar induces a higher transverse displacement to crack opening ratio as compared to a smaller diameter bar, the relative magnitude of the maximum curvature of the former is smaller because it is distributed over a larger absolute length, which is also dependent on the bar diameter (typically '4D' to '5D').

On the other hand, the effect of the higher curvature on the smaller diameter bar is essentially lower on the extreme bar fibers because of the much smaller distance between the extreme fiber and the centroid of the bar section. This trend is clearly evidenced from comparison of test results of the maximum curvature and the ultimate strength of Specimens 4 and 6, which have similar reinforcement ratios but different bar diameter, as depicted **in Fig.5**. Overall it can be said that the reduced bar axial capacity is not highly sensitive on the bar diameter. This is also verified from test results, as shown in **Fig.3(d,f),** where the reduction of axial strength for specimens 4 and 6 are similar, having nearly the same reinforcement ratio and similar concrete strengths, but different diameters for embedded bar.

(4) Mechanism of reduced axial stiffness caused by dowel action

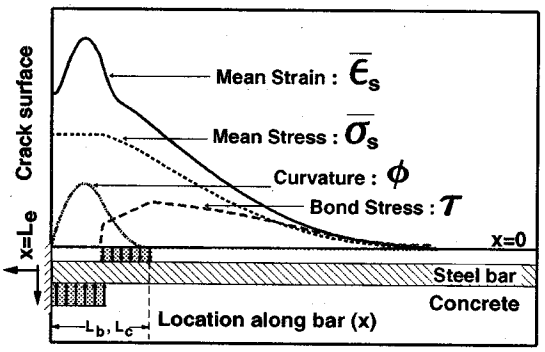

Fig.8 Schematic view of local state variables

Since the sectional mean stress and strain relation of a bar is affected by the curvature and the really induced curvature is non-uniform, complex but greater mean axial strain results, no matter how smoothly the axial mean stress may vary. As the curvature at the crack location is none due to geometric symmetry, pure axial tension is reproduced. But at the other location, the fiber strain becomes larger than the pure axial one at the crack. Once the bar attains its maximum axial sectional stress capacity at the critical maximum curvature location inside concrete, even as the section at the crack is still elastic, confinement by the bar is lost due to the total loss of stiffness, necessary to resist the bending associated with the transverse displacement.

It can be concluded that the curvature caused by the transverse shear, initiates the localized inelastic axial strain which subsequently reduces bar mean yield strength and stiffness. This mechanism is the source of the reduced anchorage performance of embedded bars under a generic coupled displacement path of axial pullout and transverse shear slip.

For the modeling of the reduced stiffness and strength of a bar under the generic displacement path, simplified distribution profiles for the curvature and the deteriorated bond stress near the crack can be assumed as shown in **Fig.8**.

4. DOWEL BEHAVIOR WITH COUPLED AXIAL PULLOUT

The capacity of an embedded bar to resist shear across its section, termed as dowel action, can be also affected by the level of axial stress applied to the bar. Though the dowel force could not be directly measured, it is possible to compute it with the beam theory and profiles of induced curvature as,

$$V(x) = \frac{dM}{dx}, \quad M = E_s \cdot I_b \cdot \phi(x) \qquad (6)$$

where, M(x), V(x) and $\phi(x)$ are the bending moment, shear force and curvature along the bar axis respectively, and E_s and I_b are the elastic modulus and moment of inertia of the bar section, respectively.

By fitting experimentally obtained curvature profiles by means of the second degree polynomial functions (the same method to calculate local bond stress by Shima et al.[2]), the shear force at a crack point by x=0 was computed. The computed shear stress (τ_s=V/A_s) carried by the bar versus the associated bar transverse displacement, taken as one half of the interface plane displacement, and the sectionally averaged mean axial stress in the bar, are plotted in **Fig.9** for typical specimens.

The dowel shear stiffness shows a linear increase in the beginning and then a gradual loss of stiffness with increasing transverse displacement and mean axial stress. The ultimate shear carried by the bar at the peak shear capacity of the interface is about one third of the pure dowel capacity of 170 MPa for a bar of 25 mm diameter and similar concrete strength, but without any associated axial stress, as reported in reference (15). This premature reduction in dowel stiffness and capacity, as compared to pure dowel performance, is brought about primarily by the coupled axial stress in the bar and also by the gradual softening of the concrete supporting the dowel due to the radial bond micro-cracks resulting from bar pullout, in addition to the crushing of concrete resulting from bar transverse displacement.

Comparison of dowel performance for Specimens 5 and 6, which have all common parameters except reinforcement ratio, clearly demonstrates the reduction of dowel capacity with the increase in axial capacity, as shown in **Fig.9(b,c).** For Specimen 5 having lower reinforcement ratio, the associated displacement path in terms of the ratio of axial pullout to transverse displacement of bar is higher than Specimen 6. Therefore, the maximum axial stress attained is higher, which reduces the dowel shear attained by Specimen 5 as compared to Specimen 6.

Theoretically speaking, if there is no transverse displacement and only axial pullout, the bar axial stress of the bar should reach the yield stress and the

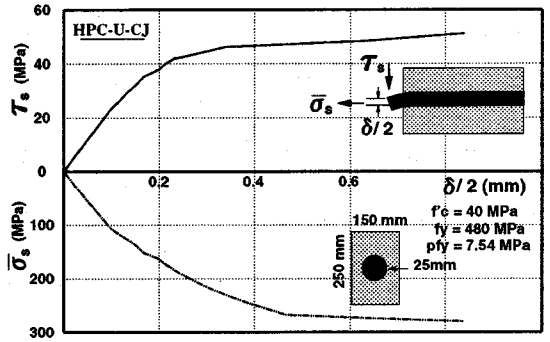

(a) Specimen 4

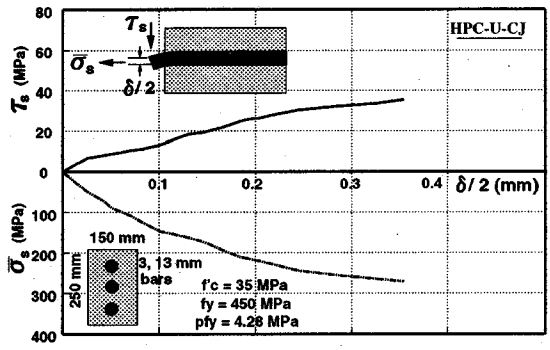

(b) Specimen 5

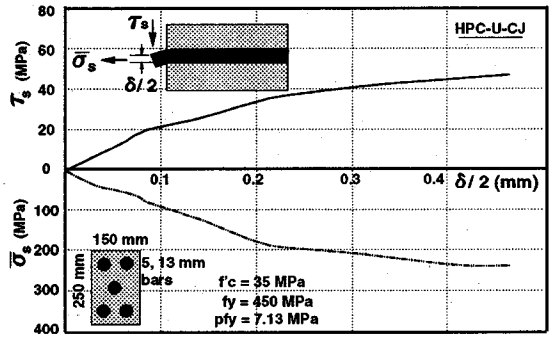

(c) Specimen 6

Fig.9 Shear stress and mean axial stress in bar versus transverse displacement

dowel shear should be non-existent. Conversely, if there is no axial pullout and only transverse displacement is applied, the axial stress will be zero and the full dowel capacity can be attained.

However, under a coupled displacement path, the pullout behavior is affected by the transverse shear, and the dowel action is in turn affected by the pullout. Thus the pullout and dowel behaviors are "mutually" interactive and strongly influenced by the local plasticity which results from the crack-steel interaction. The coupled displacement path brings about a reduction in both axial and transverse load carrying capacity of the bar, the ratio of which depends on the level of axial to transverse loads induced by the displacement path.

If the transverse displacement is high, as compared to axial pullout, the axial capacity is reduced more because of the higher dowel shear attained. If the pullout is comparatively higher, the dowel capacity is reduced more due to increased axial capacity attained as seen from **Fig.9(b,c).**

5. NONLINEAR INTERACTION WITH CRACK SHEAR IN CONCRETE

It was reported by Mishima et al.[5] that when reinforcement ratio exceeds 2%, the shear capacity of RC cracks and joints cannot be derived from mere superposition of models, verified independently, for stress transfer of plain concrete crack and one dimensional pullout model of reinforcement. In general, analytical prediction on ultimate capacity exceeds tested results, even though such predictions neglect the dowel shear carried by reinforcement.

From experiments in this study, it can be considered that a primary source of the reduced shear capacity might originate from the lowered confinement efficiency against crack opening of embedded bars due to reduced axial capacity of steel mobilized by shear slip along the crack. It will accelerate the reduction of pullout stiffness and strength in turn, finally determining the ultimate shear capacity. Mattock also reported this failure mode appearing in push-off tests[9] where the steel does not yield at the ultimate shear. But, it is much less than the shear capacity of a plain concrete crack[6] restrained by external confinement. It appears that the shear failure is governed by the failure of concrete crack plane, whereas in reality it is the failure of steel inside concrete which initiates the entire failure of load carrying system.

The shear stress, shear slip and surface crack opening relations along the flat joint planes is shown for typical specimens in **Fig.10**. Also shown are analytical results as obtained by superposing a concrete stress transfer model by Bujadham et al.[3], and a bond pull-out model by Shima[2], which does not take into account the local curvature and corresponding deteriorated anchorage performance by

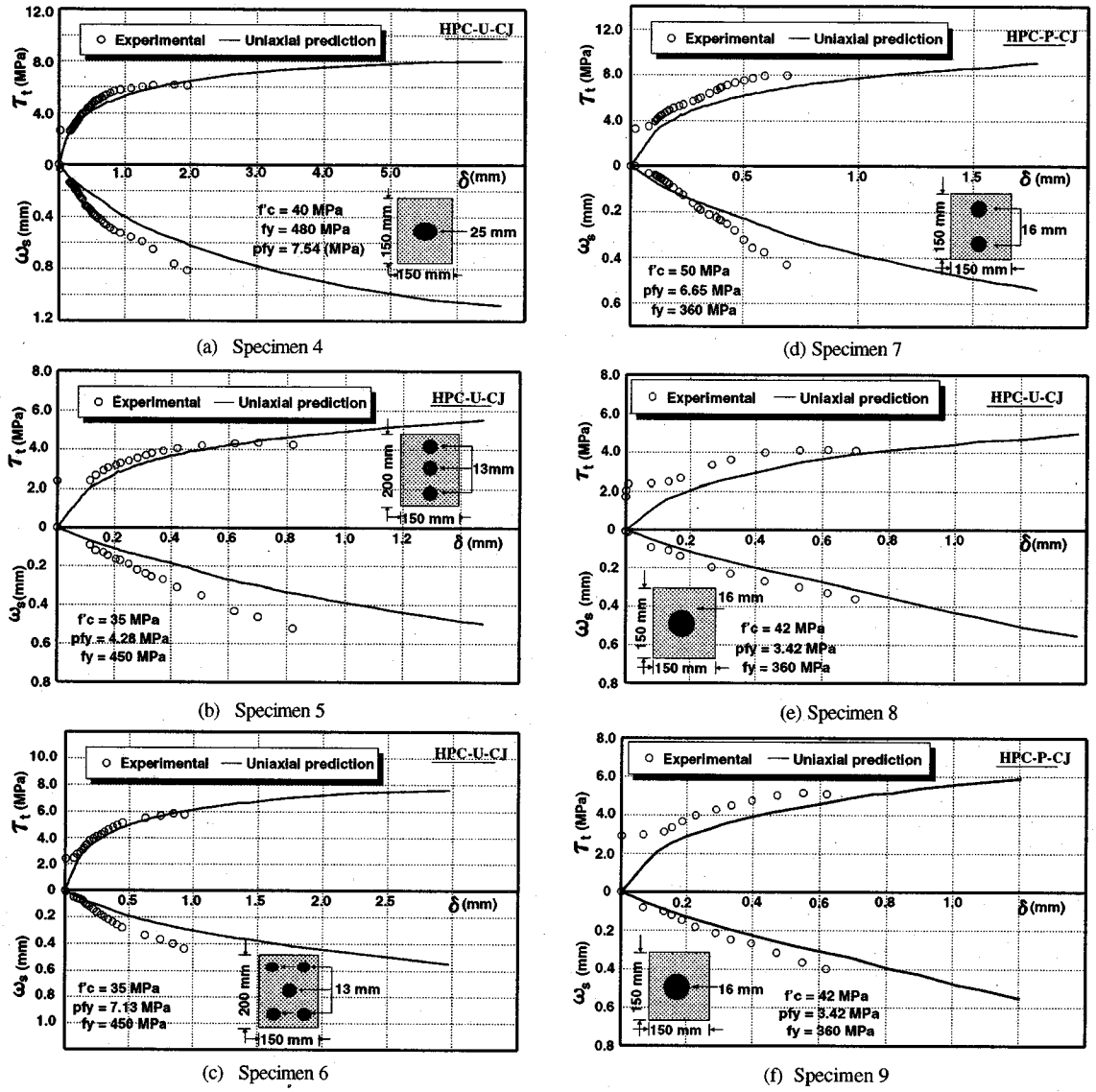

(a) Specimen 4 (d) Specimen 7

(b) Specimen 5 (e) Specimen 8

(c) Specimen 6 (f) Specimen 9

Fig.10 Comparison of analytical and experimental shear stress transferred with associated displacement paths at interface for typical specimens

steel. As shown in **Fig.10**, the shear capacity and the associated deformational paths cannot be satisfactorily predicted by the above analysis. The highly over-predicted shear slip, lower surface crack opening and higher shear capacity, even while neglecting shear transferred by dowel action, is not substantiated by the test results.

This lack of agreement between test and analysis may be explained by considering the reduced axial performance of the bar, which is subjected to a coupled displacement path in the test but only considered to be axially pulled in the analysis. The lowered bar performance would then be the major source for the reduced shear capacity and also one of the factors effecting the predicted and analytical surface crack opening (compatibility condition in analysis considers average crack opening as twice the pullout).

It has been verified from the experiments that an increase in reinforcement ratio reduces the mean axial confining stress in the embedded bars.

However, an increase in reinforcement ratio increases shear capacity, because the total confining force would be higher in case of higher ratio and also the contribution to shear transfer by dowel action would also increase. If the reinforcement ratio is low, the discrepancy between analytical (simple superposition) and experimental results would also be small, since the embedded bar would reach an axial stress close to its yield stress under pure axial tension and dowel shear, neglected in the analysis, would be small.

For larger reinforcement ratios, the over-estimation would be higher. It is however to be noted that the dowel capacity would also increase with an increase in reinforcement ratio, thereby balancing some of the variance in the total shear capacity. The true mechanism in which the two modes of shear transfer, i.e. aggregate interlock and dowel action, originating from the same displacement path defined at the interface, interact cannot be understood from the present analytical technique.

In view of this discussion, it is clear that by assuming the embedded bar to provide a interface dilatancy resisting force equal to its yield capacity, and neglecting shear force carried by the embedded bar, regardless of reinforcement ratio, material strengths and interface geometry, might bring about satisfactory predictions of interface capacity in some cases. But the true interactive mechanisms of steel and concrete are not captured, and associated displacements related to the capacity would be inaccurate for this reason. Gross inaccuracies of even capacities would result under specific cases. Therefore, for the accurate and versatile prediction of shear capacity of different RC interfaces, a generalized model incorporating bar behavior under coupled displacement paths and plane concrete stress transfer behavior under interaction with the embedded bar, is imperative.

6. CONCLUSIONS

Generic pullout behaviors of deformed steel bars embedded in concrete and subjected to axial and transverse displacements were extracted from the overall mechanics of the reinforced crack section. Within the scope of this study, the following can be concluded.

(1) In addition to the axial pullout of reinforcement due to crack dilatancy, the transverse displacement at a crack plane induces a zone of curvature in the bar. Near the crack plane, the mean stress profile shows an uniform trend, however the mean strain profile shows significant non-uniformity due to the induced localized curvature.

(2) The induced curvature reduces the axial stiffness and strength of reinforcement inside concrete due to local inelasticity arising in the bar inside concrete.

(3) The reduced axial stiffness of reinforcement causes the inelastic axial strain along the bar under the lower axial stress. This local inelasticity gives rise to greater pullout and lower anchorage performance.

(4) The reduced stiffness and strength of the confining reinforcement affects the shear capacity carried by the rough surfaces of the concrete interface. This reduction rate of this confinement is chiefly related to the displacement path to which the bar is subjected to at the interface.

(5) The dowel and pullout behaviors of embedded bar are mutually interactive and interdependent. The pullout behavior is affected by the transverse shear, and the dowel action is in turn affected by the pullout behavior. This mutual dependency is strongly influenced by the local plasticity resulting from the interaction between the interface and the embedded bar.

(6) For proposing a versatile model to predict the stress transfer behavior of a RC interface, it is crucial to formulate the reduced axial stiffness and strength model for embedded bar under coupled effect of axial pullout and transverse displacement.

In the following study, such a generic bar model would be attempted to be formulated.

REFERENCES

1) Okamura, H. and Maekawa, K.: *Nonlinear analysis and constitutive models of reinforced concrete*, Giho-do Press, Tokyo, 1991.
2) Shima, H., Chou, L. and Okamura, H.: Micro and macro model for bond behavior in reinforced concrete, *Journal of the faculty of engineering, The University of Tokyo (B)*, Vol. 39, No.2, 1987.
3) Bujadham, B., Maekawa, K. and Mishima, T.: Cyclic discrete modelling for reinforced concrete, *Computer aided analysis and design of concrete structures*, Pineridge Press, 1990, pp.1225-1236.
4) Mishima, T., Yamada, K. and Maekawa, K.: Localized deformational behavior of a crack in RC plates subjected to

reversed cyclic loads, *Proc. of JSCE*, No.442/V.-16, Feb., 1992, pp.161-170.

5) Mishima, T., Bujadham, B. and Maekawa, K.: A development of a RC discrete crack model under reversed cyclic loads and a verification of its applicable range, *Proc. of JSCE*, No.442/V.-16, Feb., 1992, pp.181-190.

6) Li, B., Maekawa, K. and Okamura, H.: Contact density model for stress transfer across cracks in concrete, *Journal of the faculty of engineering, The University of Tokyo (B)*, Vol. 40, No.1, 1989.

7) Mishima, T., Bujadham, B. Maekawa, K. and Okamura, H.: A development of constituent material models for a reinforced concrete discrete crack, *Proc. of JSCE*, No.442/V.-16, Feb., 1992, pp.171-179.

8) Bartos, P. (editor): *Bond in Concrete*, Applied Science Publishers, London, 1982.

9) Mattock, A. H. and Hawkins, N. M.: Shear transfer in reinforced concrete-recent research, *Journal of PCI*, Vol.17, No.2, March-April, 1972.

10) Mishima, T., Yamada, K. and Maekawa, K.: Discrete crack finite element analysis of reinforced concrete structures subjected to alternate force and thermal load, *Proc. of JSCE*, No.442/V-16, Feb.,1992, pp.201-210.

11) Bujadham, B. and Maekawa, K.: The Universal Model for Stress Transfer across Cracks in Concrete, *Proceedings of the JSCE*, No. 451/V-17, pp.277-287, 1992.

12) Bujadham, B. and Maekawa, K.: Qualitative Studies on Mechanisms of Stress Transfer across Cracks in Concrete, *Proceedings of the JSCE*, No. 451/V-17, pp.265-275, 1992.

13) Maekawa, K., Khan, J., Qureshi, J. and Mishima, T.: Reduced Axial Stiffness of Deformed Bars Under Shear Slip along a Crack in Concrete, *Bond in Concrete*, CEB, Latvia, Oct. 1992.

14) Yamada, K. and Aoyagi, Y.: Shear Transfer along Cracks, *Proceedings of the JCI 2nd Colloquium on Analytical Studies on Shear Design of Reinforced Concrete Structures*, JCI, pp. 19-26, Oct. 1986.

15) Poli, S. D., Prisco, M. D. and Gambarova, P. G.:Shear Response, Deformations, and Subgrade Stiffness of a Dowel Bar Embedded in Concrete, *ACI Structural Journal*, V. 89, No. 6, 1992, pp. 665-675.

16) Beedle, S. L., Ready, J. A. and Johnston, B. G.: Tests of Columns under Combined Thrust and Moment, *Proc. of Society of Experimental Stress Analysis*, Vol.8, 1950, pp.109-132.

(Received February 13, 1995)

引抜けと軸直交変位の組合せ作用を受けるコンクリート中の鉄筋挙動

前川宏一・Juneid QURESHI

本研究は，コンクリートのせん断ひび割れと交差する鉄筋の引き抜け挙動について，実験的検討を加えたものである．ひび割れ面に沿ってせん断変位が導入される場合，鉄筋軸と直交方向の変位が鉄筋に与えられる．この時，鉄筋の引抜け耐力は常に全断面降伏耐力を下回ることが実験的に示された．鉄筋軸に直交方向の変位によって鉄筋断面に曲率が導入されるため，せん断ひび割れ面から離れたコンクリート中の鉄筋断面位置が限界断面となる．そのため，低軸応力下でも鉄筋に塑性変形が発生して，鉄筋軸方向の引抜け挙動が終局に至るのである．したがって，接合面で鉄筋比が高い場合，あるいは接合面の形状が平滑な場合には，引抜けと軸直交方向変位の相互作用を，構造解析において無視できないことが示された．